Geodynamic modeling of subduction zones with low viscosity wedges: a recipe for flat slabs onset

Vlad Manea[1,2] and Michael Gurnis[2]

1 - Computational Geodynamics Laboratory, Centro de Geociencias, UNAM, Mexico

2 - Seismological Laboratory, CALTECH, Pasadena, USA

Abstract.

Dehydration of subducting lithosphere likely transports fluid into the mantle wedge where the viscosity is decreased. Such a decrease in viscosity could form a low viscosity wedge (LVW) or a low viscosity channel (LVC) on top of the subducting slab. Using numerical models, we investigate the influence of low viscosity wedges and channels on subduction zone structure. Slab dip changes substantially with the viscosity reduction within the LVWs and LVCs. For models with or without trench rollback, overthickening of slabs is greatly reduced by LVWs or LVCs. Two divergent evolutionary pathways have been found depending on the maximum depth extent of the LVW and wedge viscosity. Assuming a viscosity contrast of 0.1 with background asthenosphere, models with a LVW that extends down to 400 km depth show a steeply dipping slab, while models with an LVW that extends to much shallower depth, such as 200 km, can produce slabs that are flat lying beneath the over-riding plate. There is a narrow range of mantle viscosities that produces flat slabs (5 to10 x10^{19} Pa s) and the slab flattening process is enhanced by trench rollback. Slab can be decoupled from the overriding plate with a LVC if the thickness is at least a few 10s of km, the viscosity reduction is at least a factor of two and the depth extent of the LVC is several hundred km. These models have important implications for the geochemical and spatial evolution of volcanic arcs and the state of stress within the over-riding plate. The models explain the poor correlation between traditional geodynamic controls, subducting plate age and convergence rates, on slab dip. We predict that when volcanic arcs change their distance from the trench, they could be preceded by changes in arc chemistry. We predict that there could be a larger volatile input into the wedge when arcs migrate toward the trench and visa-versa. The transition of a subduction zone into the flat lying regime could be preceded by changes in the volatile budget such that the dehydration front moves to shallower depths. Our flat slab models shed some light on puzzling flat subduction systems, like in Central Mexico, where there is no deformation within the overriding plate above the flat segment. The lack of in-plane compression in Central Mexico suggests the presence of a low viscosity shear zone above the flat slab.

Keywords: Low viscosity; mantle-wedge; flat subduction; dip angle

Basic equations, viscosity formulation, particle tracers with low viscosity wedges and channels

The calculations are performed in a 2-D cut through a sphere on a non-deforming grid, by solving the conservation equations of mass, momentum and energy while making the Boussinesq approximation. The equations are written in non-dimensional form and the summation over indices is implicit:

$$u_{i,i}=0$$

$$P_{,i}+(\eta u_{i,j}+\eta u_{j,i})_{,j}+Ra\,T\delta_{ir}=0$$

$$T_{,t}+u_i T_{,i}=T_{,ii}+\gamma$$

The mantle is divided into four layers: lithosphere (0-100 km), upper mantle (100-410 km), transition zone (410-670 km) and part of the lower mantle (670-1300 km). The viscosity is temperature- and depth-dependent:

$\eta(r,T)=f(r)\exp(c_1/(c_2+T)-c_1/(c_2+T_m))$

f(r)= η_{LVW} and c_1=0 if inside wedge

where f(r) is a non-dimensional value that differs in each layer. The dimensional viscosity in each layer is obtained by multiplying the non-dimensional value with the reference value, $\eta_0=10^{21}$ Pa s. A non-dimensional viscosity variation of 10^4 or 0.01-100 is used across the whole domain. For our nominal set of calculations, the non-dimensional parameters were set to c_1=7 and c_2=0.1 with a viscosity cut-off of 100 and were chosen so that the dimensional viscosity of the slab did not exceed ~10^{23} Pa-s. T_m = 1 is the non-dimensional temperature of ambient mantle.

Using the finite element package CitcomS Version 2.0.1 [1] available from the Computational Infrastructure for Geodynamics (CIG) (http://geodynamics.org), the computations are performed within a thin spherical domain (r,), where r is radius and is longitude. The inner radius corresponds to a depth of 1300 km, the outer radius the surface of the Earth. The span in longitude is 57°. This domain is evenly divided into 128 elements in the radial and 640 in longitude, corresponding to a 10 x 10 km resolution. The top and bottom boundaries are isothermal. The top boundary has an imposed velocity boundary condition, the bottom is free slip, and the sides are reflecting. The initial thermal structure is described by a thermal boundary layer (age controlled) at the top and isothermal mantle with an initial slab with a 30° dip angle (Fig. 1a). A typical vertical viscosity profile is presented in Figure 1c.

A set of particle tracers (5,000) is evenly distributed on the top of the oceanic plate at a depth of 5 km and along the initial slab geometry (see Fig. 1a). Tracer velocity is calculated by interpolating the eight nodal velocities with the bilinear shape functions. Tracers are advected with the mid-point method (2nd order accuracy). Low viscosity wedges and channels are generated from the geometry of the subducted crust. We defined three parameters that control the low viscosity wedge: minimum depth (h_{MIN}), maximum depth (h_{MAX}), and wedge viscosity (η_{LVW}). The maximum horizontal extent (w) of the LVW is measured from the slab surface at h_{MAX} (Fig. 1b). We use a constant value of w of 50 km for all LVW models. For the low viscosity channels, we have a channel thickness (d_{LVC}).

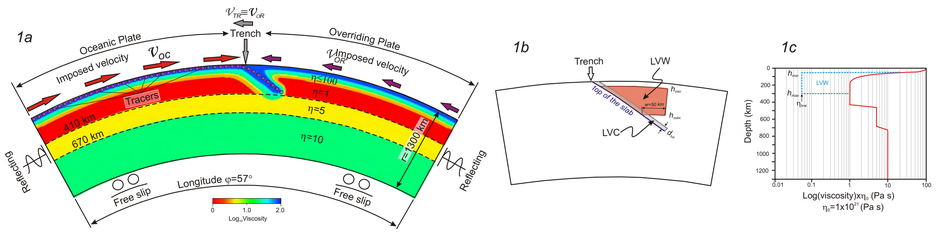

Figure 1

Model results

We find that the introduction of a low viscosity wedge above the subducting slab has a substantial effect on subduction zone structure, including slab dip. The parameters used LVW simulations presented in Figure 2 are: h_{MIN} = 40 km, h_{MAX} = 300 km, w = 50 km, η_{LVW} = 0.1. At 5 Myr after the inclusion of the LVW, higher temperature upper mantle penetrates further into the top of the mantle wedge. With the smaller resistance of the slab from the over-riding plate, the slab penetrates more deeply into the transition zone compared to the case without a LVW. By 10 Myr, the slab is not advectively thickened within the upper mantle, as it is in the models without an LVW (Fig. 2a). As subduction continues, the differences between the models increase as the slab fully penetrates into the lower mantle.

The maximum depth of the LVW (hMAX) has a strong influence on slab structure and can cause slab dip to change substantially for depths <150 km (Fig. 3). For shallow LVW (200 km) the slab has a small, ~10°, dip within the 50 to 100 km depth range . This model shows a ~100 km flat slab segment located from 200 to 300 km from the trench (Fig. 3a). Increasing the depth extension of the LVW (400 km) gives rise to a steeper slab (Fig. 3b). In other words, when the low viscosity wedge is shallow, it tends to promote flat flying subduction.

The pressure distribution provides insight on the relationship between slab dip and the LVW. As shown for two models, LVW=1.0 and 0.1 (Fig. 4), although the initial conditions are the same (see Fig. 1), the pressure distribution above the slabs differs considerably after 20 Myr of convergence. With a high wedge viscosity, there is a region of negative pressure greater than 200 MPa (Fig. 4a, inset), but the size of this region decreases considerably as the scaled mantle wedge viscosity decreases from 10^{21} Pa s to 10^{20} Pa s. The models show a bimodal pressure distribution: positive pressure beneath the subducting slab, and negative pressure above the slab. The high negative pressure for models with high wedge viscosity pulls the slab to shallower depth so that the slab has small dip angles. Models with a LVW reduces the suction force occuring in the depth range between 100 to 300 km depth allowing the slab to more evenly descend into the lower mantle.

We also introduced trench rollback in our models, the rate of trench migration being equal to the overriding plate velocity, and is a constant 2 cm/yr. The mantle viscosity within the wedge was also reduced in these models (h_{MIN} = 40 km, h_{MAX} = 300 km). The results show that a reduction by a factor of two in the wedge viscosity (η_{LVW}=0.5) produces a perfectly flat slab after 20 Myr (Fig. 5a). When the wedge viscosity is decreased further (η_{LVW}=0.05), the slab dip increases (Fig. 5b), even in the presence of trench rollback. The maximum depth of LVW (h_{MAX}) also significantly influences slab geometry. Keeping wedge viscosity constant (η_{LVW}=0.1), while decreasing h_{MAX} from 400 km to 200 km, the slab dip is reduced considerably for depth of 50-100 km. We obtain a flat slab when the maximum depth extent of LVW is reduced to 200 km.

Discussion and Conclusions

With time-dependent models, we showed that LVWs and LVCs have a significant influence on slab evolution. We show that a LVW with a viscosity an order of magnitude smaller than the upper mantle produces different slab geometries for different LVW maximum depths. It is essential that there must be a localized viscosity reduction for the wedge to influence slab dip. Merely reducing the upper mantle viscosity or thinning the thickness of the over-riding plate does not effectively influence slab structure. For example, a shallow LVW (h_{MAX}=200 km) produces a flat slab structure, whereas extending the LVW down to 400 km, a steeper slab geometry is obtained. The same pattern is obtained by using different viscosity reductions in the mantle wedge above the slab. Introducing only a small reduction in the mantle wedge viscosity (50%), a flat-slab geometry emerged, but reducing the wedge viscosity even more (20° times less than the upper mantle viscosity), moderately steepens the slab. This suggests that if flat-lying subduction is caused by reduced wedge viscosities, then only a narrow range of viscosities will give rise to the phenomena. Finally, the models may have important implications for the state of stress within the over-riding plate when slabs are in the flat lying regime. We predict that in some cases, there should be efficient decoupling between the slab and over-riding plate. Some flat lying subduction systems place the over-riding plate into compression. This would imply a strong coupling between the flat slabs and overriding plate. However, in Central Mexico, there is no evidence for in plate compression above the flat lying subduction [46-48]. It is possible that there are different causes for flat lying subduction. We conclude that the lack of in-plane compression in Central Mexico would suggest the presence of a low viscosity shear zone located above the flat slab.

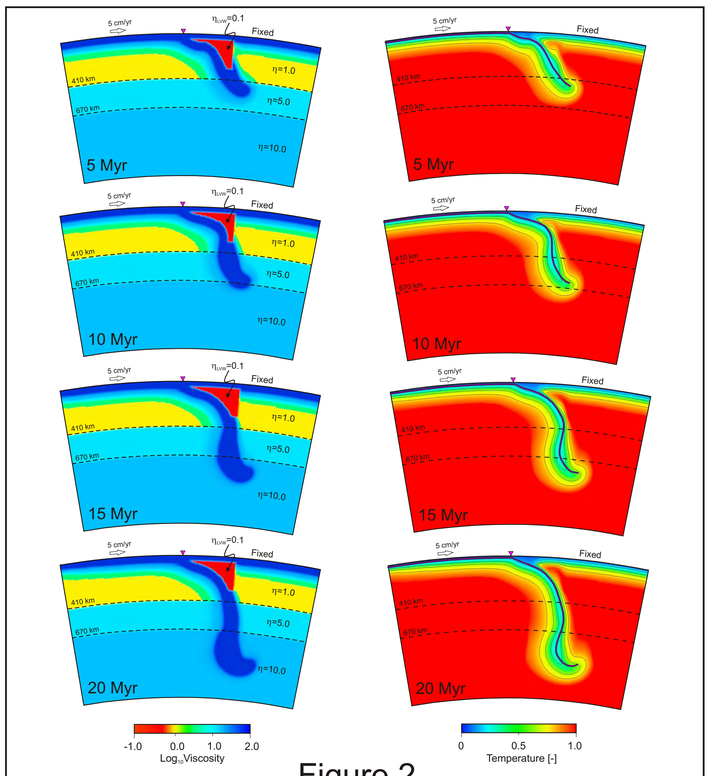

Figure 2

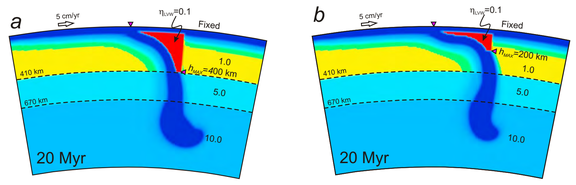

Figure 3

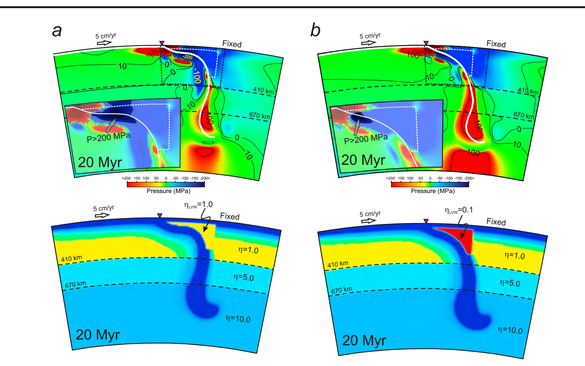

Figure 4

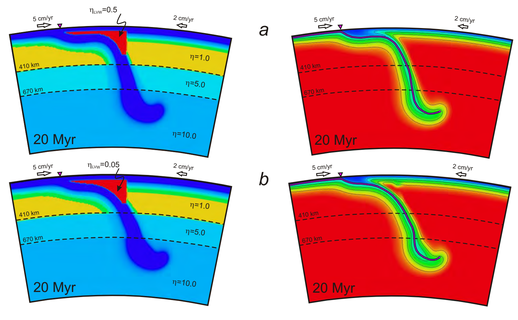

Figure 5

[1] Tan, E., E. Choi, P. Thoutireddy, M. Gurnis, and M. Aivazis, GeoFramework: Coupling multiple models of mantle convection within a computational framework, Geochemistry, Geophysics, Geosystems, 7, Q06001, doi:10.1029/2005GC001155, 14 pp., 2006.

[2] M. Cerca, L. Ferrari, M. Bonini, G. Corti and P. Manetti, The role of crustal heterogeneity in controlling vertical coupling during Laramide shortening and the development of the Caribbean-North America transform boundary in southern Mexico: insights from analogue models. Special Publication of the Geological Society, London. n. 227, (2004), 117-140.

[3] A. Nieto-Samaniego, S. Alaniz-alvarez, G. Silva-Romo, M.H. Eguiza-Castro, C. Mendoza-Rosales, Latest Cretaceous to Miocene deformation events in the eastern Sierra Madre del Sur, Mexico, inferred from the geometry and age of major structures. Geological Society of America Bulletin, 118, (2006), 238252, doi: 10.1130/B25730.1.